Standard Issue – Article

Journal of Agricultural Engineering

https://www.agroengineering.org/

Real-time straw moisture content detection system for mobile straw granulator

Wei Wang, Yuanjuan Gong, Xuewei Bai, Rui Tan

Please cite this article as doi: 10.4081/jae.2024.1570

Submitted: 30/12/2022
Accepted: 20/02/2024

Real-time straw moisture content detection system for mobile straw granulator

Wei Wang,[1,2] Yuanjuan Gong,[2] Xuewei Bai,[2] Rui Tan[2]

[1]College of Information Science and Engineering, Shandong Agricultural and Engineering University, Jinan; [2]College of Engineering, Shenyang Agricultural University, Jinan, China

Correspondence: Wei Wang, College of Information Science and Engineering, Shandong Agricultural and Engineering University, Jinan 250100, China.
E-mail: wangwei2022edu@163.com

Key words: detection; frequency; mobile straw granulator; moisture content; water replenishment module.

Conflict of interest: the authors declare no potential conflict of interest.

Funding: none.

Abstract

In order to improve the molding rate of biomass particles extruded by ring mold of the mobile straw granulator, a real-time straw moisture content detection system based on frequency was designed in this paper. The detection system comprised the frequency based acquisition devices and the supporting circuits, and support vector regression (SVR) based calculation method. The acquisition device contained a soil separation cylinder and a signal detection chamfer. The soil separation cylinder was used to remove the soil from the straw. The moisture of the straw was transformed into the relatively stable frequency for detection, but the temperature can affect the Brownian movement of free water. Hence, the designed signal detection chamfer mainly contained a frequency sensor and a temperature sensor. The proposed calculation method blended the frequency and temperature to acquire the accurate moisture of the straw. A water replenishment module was also designed to verify the effectiveness of the detection system, and it was used to supply water to the straw when it becomes too dry. The system was verified in the experimental plots and field. The actual moisture content was obtained by 105℃ drying method. The results obtained in the experiment plots showed that the detectable moisture content range was between 9.09% to 46.68%, the maximum detection error was less than 0.44%, and the average absolute error was less than 0.33%, and the molding rate could reach approximately 94%. The results obtained in the fieldd showed that the average molding rate achieved was 93.57% and 89.76% for straws with moisture content of about 20% and 15%, respectively. The detection system comprehensively takes into account the influence of temperature and soil on moisture content and can effectively improve the working efficiency of the mobile straw granulator.

Introduction

Due to the growing awareness of environmental protection and the pressure of resource scarcity, biomass particles, as a renewable energy alternative to traditional energy sources, have garnered increasing attention. Moreover, converting the straw into biomass particles is suitable for farmers as they can directly store them for winter heating and the price of granulation equipment is reasonable. The quality of biomass particles is related to their combustion efficiency, environmental protection, safety, and other aspects. Additionally, the quality of biomass particles can reflect the operating status of the equipment. Consequently, the quality requirements for biomass particles are becoming increasingly high. Moisture content is a crucial factor that affects the molding rate of biomass particles, i.e., both excessively high and low moisture content can adversely impact the quality of biomass particles (Sun, 2020; Thais *et al*., 2021). This can be mitigated by controlling the moisture content of the straw entering the ring mold. Currently, the methods of moisture detection mainly include radio frequency, capacitance, neutron, microwave and nuclear magnetic resonance techniques (Jain *et al*., 2020; Abdullah *et al*., 2019; Lv *et al*., 2018; Han *et al*.,2023). Each detection method has its own strengths and limitations. Microwave and infrared have a significant impact on the shape, thickness, and density of the tested object. The neutron method's measurement accuracy depends on the stability of hydrogen scattering characteristics, while the nuclear magnetic resonance method is costly. Among them, the capacitance method has often been adopted by many researchers due to its good dynamic performance, simple plate structure, low cost and easy implementation of sampling circuit principle (Fan *et al*., 2020; Li *et al*., 2021; Fan *et al*., 2022). Using the sampling bench, an online detection system for rice moisture content in combine harvesters is designed using capacitance method, and satisfactory results are achieved (Wang *et al*., 2021). A low-cost wireless device designed to measure changes in rice moisture content around silos can detect multiple levels of localized moisture distributions, albeit with a limited detection range and slow detection speed (Almaleeh *et al*., 2022). Scholar Chen (Chen *et al*., 2018) developed a high frequency capacitor circuit to monitor the moisture content of the grain, but it did not account the influence of the temperature and impurities. Relevant research findings indicate that impurities have a certain impact on the accuracy of grain moisture detection. Therefore, it is essential to remove impurities unrelated to the detection process during moisture detection (Wang *et al*., 2020; Li *et al*., 2021). There are other similar moisture detection methods such as live fuel moisture content (Wang et al., 2023), flowing grain moisture contents (Yigit et al., 2022), maize grain moisture (Wang et al., 2019), and so on. Current research mainly focuses on the detection of moisture content of the grain, and there are few studies on the detection and control of moisture content of the straw.

In this paper, a real-time system was designed to detect the moisture content of the straw fed into the ring mold of the mobile straw granulator. It can acquire the moisture content of the straw in real-time, judge whether to replenish water, and calculate the water quantity according to the moisture content. A soil separation cylinder was designed to remove the soil from the straw, as the primary impurity in the straw comprises soil. The system utilizes the capacitor plate to convert the moisture content of the straw to an electrical signal. Then, the electrical signal can be transformed into frequency which can be acquired easily. A moisture content calculation method based on Support Vector Regression (SVR) was designed, and the water replenish model that depends on the moisture content and feeding amount was established. Furthermore, experiments are conducted to investigate the influence of temperature and soil, as well as experiments in plots and field conditions, to evaluate the system's performance from various aspects.

Materials and Methods

Scheme design of the overall system

The modules and workflow of the experimental mobile straw granulator are illustrated in Figure 1. During the operation of the granulator, the straw is crushed and collected by the front pickup device. Then, the straw is transported to the screw conveyor and fed to the conveying fan equipment. Driven by the mechanical equipment which can convert the mechanical energy into wind energy, the straw material is propelled through the conveying pipeline and into the silo of the granulator. under the pressure of the ring mold, the straw is squeezed to form biomass particles in cylindrical shape with an average length and diameter of 11 and 3.2 centimeters, respectively.

The condition of the straw entering the ring mold has a great impact on molding rate of the biomass particles. The molding rate refers to the proportion of normal particles with a smooth surface, uniform length, and no coking phenomenon. If the moisture content is low, meaning the straw is overly dry, the biomass particles discharge slowly, the particle surface is smooth, and some particles exhibit coking, as depicted in Figure 2A. If the moisture content is normal, the granulation speed will be fast, the particle surface is smooth, there is no coking phenomenon, and the particle length is uniform, as illustrated in Figure 2B. If the moisture content is high, meaning the straw is too wet, the particles are fragile, with cracks on the surface and uneven length, as shown in Figure 2C. To ensure that the straw has normal moisture content, this paper designed a moisture content acquisition module in the silo of the granulator. This module samples straw materials in real-time and detects the moisture content through an electronic circuit. It analyzes the moisture content of straw samples and activates the water replenishment module to add water to straw with low moisture content, thus ensuring proper moisture content. Further, straw materials with high moisture content should undergo natural air drying before processing.

The block diagram of the real-time moisture content detection system and the water replenishment module is shown in Figure 3. The moisture content detection system is composed of straw sampling module, soil removal module, temperature detection module and frequency detection module. The straw sampling module focuses on collecting and transferring the straw. The soil removal module separates the soil from the straw samples, and the outcomes are exhibited on the liquid crystal display (LCD). The water replenishment module primarily adds water to the straw with low moisture content to enhance the straw's moisture content. The Main control unit (MCU) serves as the core signal dispatching and data storage module, integrating calculation and analysis functions.

Design of the straw moisture detection system

Design of moisture content acquisition device

The schematic diagram and the actual instance of moisture content acquisition device are presented in Figure 4A and 4B, respectively. The device primarily consists of straw samples inlet, stepping motor, small screw conveyor, soil separation cylinder, signal detection chamber, pressure detection device, capacitor plate and straw samples outlet. The pressure detection device is designed to detect the compactness of straw in the chamber. When the pickup and crushing device works, the crushing knife, straw, and the field will interact with each other, and lead to the soil of the field enter the screw conveyor, fan and conveying pipeline together with the straw. Therefore, the soil separation cylinder is designed to separate soil from the straw samples. The stepper motor M3 shown in Figure 4A drives the small screw conveyor to rotate and transfer the straw collected in the material inlet to the signal detection chamber. The type of M3 stepper motor is 86BYG250H with an output torque of 12 N·m and a speed of 200 r/min. When the straw material in the chamber is extruded to about 10N pressure and compacted, the detection module executes the acquisition of frequency signal. Subsequently, the extrusion force pushes the two semicircular baffles, controlled by two springs, away, and the straw samples falls into the large silo. In the process of transportation, the soil will be removed through the soil separation cylinder. During the operation in the field, water evaporation will increase rapidly with the rising temperature. To examine the influence of soil content and temperature on moisture content, a pilot experiment was carried out in Section 3.1. The results indicated that soil content does affect the accuracy of moisture content measurement. Consequently, the straw sampling device incorporates a soil separation cylinder to remove soil to ensure the detection accuracy.

The signal detection chamber, shown in Figure 4, is the core device for moisture content detection. It consists of capacitor plates that generate varying capacitances based on the moisture content of the straw samples. The capacitance is then converted into frequency through LC oscillation circuit (Park and Choi, 2021) to distinguish different moisture content. To achieve accurate measurement while reducing costs, the conversion adopts MC1648 semiconductor chip (Sivtsov and Khandetskyi, 2015). The capacitive plate sensor is designed as a square and primarily consists of two pieces of red copper. According to the literature research findings, the edge effect is inversely proportional to the plate spacing and plate thickness, but directly proportional to the effective area of the plate (Agrawal *et al*., 2021). In order to reduce the edge effect of the capacitor plate and include the influence of the fluidity of straw in the detection chamber, the distance between the two electrode plates is set to 60mm, and the length of the electrode plate is 90mm. The capacitive plate is inserted along the long hole on the side of the protective shell. Once the wire on the pole plate is led out, it is sealed with waterproof glue.

Electronic design of main sensor modules

The Frequency Sensor of the moisture content detection module is shown in Figure 5A. Integrated chip MC1648 (U2) has automatic gain control internally, enabling stable frequency output. C2 represents a capacitor composed of two red copper plates. Inductance L1 (820nH) and capacitors C1 and C23 are connected in parallel to form a resonant circuit. Based on the moisture content of the straw material detected by capacitor C2, the output frequency of MC1648's out terminal continuously varies, with C6, C7, and C8 serving as filters. The voltage signal output by MC1648 is input to frequency divider MC12080 for frequency division after passing through capacitor (C11). The frequency division mode is determined by SW1, SW2 and SW3. SW1 and SW2 are set to high level through R11 and R13, while SW3 is suspended, indicating a 1/20 frequency division of the input voltage signal (Gurol *et al*., 2022). U5 TLV3201 converts the non-standard sine into a standard square wave. The single-chip microcomputer collects the frequency of square wave signal and obtains the moisture content through the analysis of the frequency signal.

Main control module is shown in Figure 5B. STM32F103C8T6 (U0) (Kane *et al*., 2022) is utilized to communicate information and control the coordination of various modules. The peripheral is equipped with a clock circuit Y1 (8MHz), reset circuit P3, program download interface P1 and power filter circuit (C7, C8, C9, C10). The screen employs TFT 2.8-inch LCD HT028PQV005NH (U01) with a working voltage of 3.3V and a working current is 5mA. The backlight of the screen is controlled by MCU through an S8050 triode. The communication between the MCU and the screen utilizes 8080 sequence.

Moisture content detection method

(1) Basic Theory of Moisture Content Detection

When the movement of straw in the signal detection chamber is stable, the capacitance detected by the capacitance plate can be expressed as follows in Eq. 1,

$$C = \frac{S\varepsilon_0\varepsilon_r}{l} \tag{1}$$

where

S = relative area of plate (m^2).

ε_0 = dielectric constant of vacuum medium.

ε_r = dielectric constant of straw material.

l = relative distance between plates (m).

In the detection process, the material between the two plates is composed of dry straw, moisture, and air, which can be regarded as an equivalent model composed of solid phase, liquid phase and gas phase (Basok *et al.*, 2021). The total relative area between the plates is shown in Eq. 2,

$$B = B_1 + B_2 + B_3 \tag{2}$$

where

B_1 = equivalent relative area of dry straw (m^2).

B_2 = water equivalent relative area (m^2).

B_3 = air equivalent relative area (m^2).

The relative dielectric constant of materials between plates can be expressed as Eq. 3 as follows,

$$\varepsilon_r = \frac{B_1}{B}\varepsilon_1 + \frac{B_2}{B}\varepsilon_2 + \frac{B_3}{B}\varepsilon_3 \tag{3}$$

where

ε_1 = relative dielectric constant of dry straw.

ε_2 = relative dielectric constant of water.

ε_3 = relative dielectric constant of air.

Replace Eq. 3 with Eq. 1, the capacitance can be get as following,

$$C = \frac{S\varepsilon_0}{l}\left(\frac{B_1}{B}\varepsilon_1 + \frac{B_2}{B}\varepsilon_2 + \frac{B_3}{B}\varepsilon_3\right) \quad (4)$$

where B_3/B can be seen as the pore ratio of grain between plates and can be expressed by e.

Set the density and the mass of dry straw are ρ_1 and m_1, the density and the mass of water are ρ_1 and m_2. The moisture content of straw can be expressed as following,

$$w = \frac{m_2}{m_1 + m_2} \times 100\% = \frac{\rho_2 B_2}{\rho_1 B_1 + \rho_2 B_2} \quad (5)$$

As the density of water is 1, Eq. 6 can be obtained from Eq. 4 and 5 as following,

$$C = \frac{\varepsilon_0 B}{l}(\varepsilon_2 - \varepsilon_1) \times \frac{w\rho_1}{1 + w(\rho_1 - 1)} + \frac{\varepsilon_0 \varepsilon_1 B}{l} + \frac{\varepsilon_0 \mathrm{e} B}{l}(\varepsilon_3 - \varepsilon_1) \quad (6)$$

In LC resonant circuit, the frequency can be obtained from the inductance value L and capacitance value C as following,

$$f = \frac{1}{2\pi\sqrt{LC}} \quad (7)$$

Replace C with Eq. 6, the frequency can be expressed as following,

$$f = \frac{1}{2\pi\sqrt{L\left(\frac{\varepsilon_0 B}{l}(\varepsilon_2 - \varepsilon_1) \times \frac{w\rho_1}{1 + w(\rho_1 - 1)} + \frac{\varepsilon_0 \varepsilon_1 B}{l} + \frac{\varepsilon_0 \mathrm{e} B}{l}(\varepsilon_3 - \varepsilon_1)\right)}} \quad (8)$$

According to Eq. 8, the frequency is related to the moisture content of straw. The moisture content of straw can be detected by designing relevant electronic circuits to measure the frequency generated by LC resonant circuit.

(2) The Preprocessing Sep Based on Kalman Filtering

When the temperature rises, the Brownian movement of free water and the orientation motion of polar molecules within the straw will intensify (Zhou *et al*., 2021). Consequently, the influence of temperature needs to be considered. Thus, the moisture content calculation method based on the frequency and temperature is proposed in this paper. The frequency and temperature collected by the sensors are unstable with noise due to the vibration, dust and so on. To mitigate this issue, a preprocessing step utilizing Kalman filtering is employed to minimize the influence of noise.

The sensors acquire data at regular time intervals, resulting in the obtention of frequency and temperature sequences. Kalman filtering can estimate the state of dynamic system from a series of data with measurement noise (Hartley *et al*., 2020). Therefore, it can be applied to mitigate the noise produced by hardware and unstable factors. Figures 6A and 6B illustrate examples of frequency and temperature filtering, where the data before and after filtering are represented in cyan and red colors, respectively. It can be observed that the data burr is reduced, and the data becomes relatively stable.

(3) SVR Based Moisture Content Computing Model

SVR is derived from support vector machine (Sayari *et al*., 2021). It can solve the problems such as small sample sizes, nonlinearity, high dimensionality, local minima, nonlinear regression and so on. Hence, it is employed in this paper to estimate the moisture content. The data samples can be denoted as ($\boldsymbol{x_i}$, y_i), in which, i represents the order, $\boldsymbol{x_i} = [f_i, t_i]$ is the input vector composed of frequency and temperature, y_i is the output variable, i.e., the moisture content denoted by w_c. The input samples are mapped into the high-dimensional feature space through function ϕ, and a linear model is subsequently established to estimate the regression function. The linear model can be expressed as Eq. 9 in which $\boldsymbol{w}$ and b denote the weight vector and the threshold, respectively. The insensitivity loss function is introduced to represent the error between the observed value y_i and the prediction value f ($\boldsymbol{x_i}$, w). Function f can be obtained by minimizing the error.

$$f(\boldsymbol{x}_i, w) = w \cdot \phi(\boldsymbol{x}_i) + b \tag{9}$$

The solution to Eq. 9 can be obtained by transforming the objective function of the SVR model into a quadratic programming problem, employing Lagrange function optimization and solving the resulting duality (Anand *et al*., 2020). This can be expressed as Eq. 10, where α_i denotes the Lagrange multiplier, l_{sv} denotes the number of the support vectors, and $K(\boldsymbol{x_i}, \boldsymbol{x})$ is the kernel function.

$$f(\boldsymbol{x}, w) = \sum_{i=1}^{l_{sv}} (a_i + a_i^*) K(\boldsymbol{x}_i, \boldsymbol{x}) + b \tag{10}$$

The radial basis function (RBF) kernel (Jafarpisheh *et al*., 2020) is adopted in this paper to express the inner product in the high dimensional space as the inner product in the low dimensional space. It can be expressed as Eq. 11 in which γ is the kernel parameter.

$$K(\boldsymbol{x}_i, \boldsymbol{x}) = \exp\left(-\gamma \|\boldsymbol{x} - \boldsymbol{x}_i\|^2\right) \tag{11}$$

Design of the water replenishment module

Design of water replenishment device

For straw with lower moisture content than the proper range, a water replenishment device was designed to add water, as shown in Figure 7. This device comprises of a water replenishment tank, an electric control water valve, and a water replenishment nozzle, as shown in Figure 7A, 7B, and 7C, respectively. The electric control water valve controls the water output from the tank according to the calculated replenishment water volume. The water replenishing nozzle is placed above the silo of the granulator. The main shaft of the ring mold rotates to fully mix the dry straw and water for granulation. The water replenishment tank and electric control water valve are placed outside the silo of the granulator.

Water replenishment model

The water replenishment model is employed to replenish water to the straw with low moisture content, ensuring that the dry straw is moistened to the appropriate range before entering the ring mold. A feeding amount detection device (Wang *et al.*, 2021) is installed on the agricultural machinery to monitor the feeding amount in real-time. The water replenishment model determines whether water needs to be added according to the moisture content of straw, and determines the water replenishment amount according to the feeding amount, detected moisture content, and the optimal moisture content. The unit of feeding amount and the water replenishment amount is kg/s.

The straw entering the silo can be regarded as t a mixture of dry straw and water. Therefore, the feeding amount can be decomposed into the dried straw and water that enter into the equipment in unit time. Set the feeding amount as m_t (kg/s), the mass of the dried straw and water in unit time as m_s and m_w, they have the following relationship,

$$m_t = m_w + m_s \quad (12)$$

Set the detected moisture content as w_{in} which can be expressed as

$$w_{in} = \frac{m_w}{m_w + m_s} \quad (13)$$

Set the optimal moisture content as w_b, the mass of the water needed to be replenished in unit time as m_x. w_b can be expressed as

$$w_b = \frac{m_w + m_x}{m_w + m_s + m_x} \quad (14)$$

m_x can be obtained by combining the Eq. 12 - 14 as following,

$$m_x = \frac{w_b - w_{in}}{1 - w_b} m_t \tag{15}$$

In all, the mass of the water needed to be replenished in unit time can be denoted as the water replenishment amount, i.e., m_x (kg/s) in Eq. 15.

Results and Discussions

Pilot tests

Using constant temperature and humidity box and the sensors designed in this paper, the straw was maintained at 20% moisture content. The influence of different soil contents and temperatures on the frequency is tested, as shown in Figure 8A. It can be seen from the figure that when the soil content is less than 5.0%, the detection of the moisture content mainly relates to the temperature and the influence of the soil is small. When the soil content increases, the gap of the straw in the signal chamber will decrease, so that the relative dielectric constant of straw will increase, the capacitance value will increase and the frequency will decrease. When the temperature increases, it will accelerate the Brownian movement of water molecules in straw and the orientation motion of polar molecules, so that the relative dielectric constant of straw will increase, the capacitance value will increase and the frequency will change significantly. Therefore, this paper designed the soil removal module and temperature detection module.

In order to analyze the performance of the soil separation cylinder, an experiment was conducted using straw with soil content ranging from 0.5% to 12%. Six tests are carried out on samples with different soil content, and the rotating speed of the motor is set to 120r/min. The results are presented in Figure 8B. The soil content after soil separation by the sampling device is less than 2.4%. According to the soil influence experiment, when the soil content is less than 5.0%, it has little impact on the frequency. Therefore, this soil separation cylinder can meet the requirements of the detection.

Parameter training of moisture content calculation method

The measuring range of the sensor is obtained by spraying different amounts of moisture on the straw. The 105°C drying method (Amer *et al*., 2019; Vidal *et al*., 2022) is employed to measure the actual moisture content. The sensors are calibrated after installed to acquire the upper and lower limits of the moisture content. Silk straw of different groups is sprayed with different amount of moisture, and placed for 5 hours to allow the silk straw fully absorb the moisture. The actual moisture content is detected by the 105°C drying method. The temperature is set at 5°C~35°C with an interval of 5°C. Some experimental data were shown in Table 1, in which, “MC” denotes moisture content detected by the 105°C drying method. The first column and the first line represent moisture content and temperature respectively, and other values are corresponding frequency with MHz as the unit. The grid search (Tran *et al*., 2022) was used to get the optimal parameters of SVR. The optimal kernel parameter of RBF function and the optimal penalty factor of the loss function were obtained as γ = 0.132 and C = 44.89 respectively.

Experiment and discussion in experiment plots

Moisture content detection and soil removal performance experiments

In order to verify the performance of the detection device, silk straw collected after corn harvest in the field was used. The silk straw of different group numbers was sprayed with different amount of moisture, and placed for 5 hours to allow the silk straw fully absorb the moisture. For each group, three evenly distributed points were selected for sampling, with each point sampling approximately 50 grams (NAMSTC, 2013), and this sampling method was also adopted in the following similar experiments. The average moisture contents measured by 105 °C drying method of six groups of samples were 10.12%, 20.67%, 26.28%, 32.62%, 38.42% and 40.54% respectively. Different amount of soil was doped with the silk straw to make the soil content between 1% ~ 8% to test soil removal performance. The silk straw was then evenly added to the detection device to detect the moisture content, with the motor speed set at 120r/min. Each group of experiments was repeated for 5 times, and the average values are shown in Table 2.

From Table 2, it can be observed that the average absolute error of straw moisture content detected by the designed system is within 0.33%, and the maximum absolute error is 0.44%. When the moisture content is less than 30%, the detection error is small, while for moisture content above 30%, the error is slightly larger. After passing through the soil separation cylinder in the detection device, the soil content of the straw is reduced to less than 1.72%, indicating a significant effect of the soil removal module. Considering the conclusion of the pilot test that the influence of the soil is small when the soil content is less than 5.0%, soil separation cylinder is useful. The detection results of this system are relatively stable and it can meet the requirements of granulator for moisture acquisition.

Overall system experiment

In order to verify the effect of this system on improving the efficiency of mobile straw granulator, the granulation effect experiment of dry straw supplemented with water was carried out in this paper. From the instruction of the experimental equipment, the optimal moisture content range for the straw is between 20.06% and 23.09%. Therefore, the optimal moisture content w_b is chosen as 21.57%, and the water replenishment amount is calculated using to Eq. 15. Similarly, silk straw harvested in the field was used. The silk straw of different groups was sprayed with different amounts of water and placed for 5 hours to allow the straw filaments fully absorb water. The averaged moisture contents measured by the 105℃ drying method of the four groups of samples were 9.58%, 11.91%, 14.22% and 18.28%, respectively. The experimental results presented in Table 3 demonstrated that the moisture content of straw after water replenishment fell within the appropriate range, and the straw molding rate after water replenishment is approximately 94%, indicating that the water detection system, water replenishment model, and water replenishment device are effective.

Field experiment and result analysis

In order to verify the feasibility of the straw moisture content control system designed in this paper, the field experiments were carried out with the equipment provided by Liaoning Ningyue Agricultural Machinery Equipment Co., Ltd. in Heishan County, Liaoning Province on October 20, 2022 and October 22, 2022, respectively. The equipment used is shown in Figure 1.

The experiment conducted on October 20, 2022, focused on testing the detection effectiveness and molding rate of straw with moisture content within the appropriate range, which did not require water replenishment. The developed straw moisture content detection device was installed on the mobile straw granulator, and moisture content detection was carried out 3 times every second. The running speed of the mobile straw granulator is 0.45m/s, with the motor speed set at 120r/min. The collection bag was bound at the discharge outlet of the detection device. Once the detection was done, the equipment was stopped and the collection bag was taken out. It was used for subsequent 105℃

drying method to detect the actual moisture content of the used straw. The detection operation was repeated 6 times to get the average measured value by the sensor and it was compared with the result of the 105°C drying method. The results were shown in Table 4, in which, “Fre”, “Tem”, and “Abs-E” denoted frequency, temperature, and absolute error respectively. The experimental results showed that the average absolute error of straw detection was approximately 0.36%, with a maximum absolute error is 0.45%. Moreover, the average straw molding rate with moisture content within the optimal range is around 93.57%, The results showed that the system was reliable and stable.

The experiment conducted on October 22, 2022, focused on testing the water replenishment effectiveness and overall performance of the designed system for straw with low moisture content. It needed to replenish water to the proper range to test the replenishment effect of the designed system and the overall performance of it. Similarly, moisture content was detected 3 times every second, with a running speed of 0.45m/s, and motor speed set at 120r/min. The collection bag was bound at the discharge port of the detection device, the straw before and after water replenishment was collected. The water replenishment amount was calculated using Eq. 15 according to the moisture content and feeding amount before water replenishment. Then, the moisture content was detected by drying method. At the same time, the biomass particles were collected to calculate the molding rate of the granulator. The experimental results were shown in Table 5. As shown in the table, the absolute error between the designed detection system and the 105°C drying method is approximately 0.34%, and the average molding rate is 89.76%.

The results indicate that the system can accurately replenish water for straw with low moisture content, raising the moisture content to the appropriate range and achieving a high molding rate. Compared with the results in the experimental plots, the absolute error of the field experiment is slightly larger and the molding rate is slightly lower. This was mainly due to the presence of more soil mixed with the straw during harvest, as well as adverse conditions such as mechanical vibration. To improve the accuracy of moisture content detection, relevant soil removal devices and damping devices can be optimized.

Conclusions

In this paper, a real time detection system of moisture content of the straw entering into the mobile straw granulator was designed. The significances are embodied in three aspects. Firstly, the frequency based moisture content detection device was designed. The soil removal module could reduce the influence of the impurity. The signal detection chamfer could detect the frequency and temperature in real-time. Secondly, the corresponding moisture content calculation method was constructed based on the Kalman filtering and SVR. The moisture could be obtained accurately with the calculation method. Finally, the pilot experiment of soil and temperature, the soil removal performance experiment, and the performance experiments in experimental plot and field were performed. The experiments showed that the designed system in this paper can satisfy the final aim to adjust the moisture content of the straw to a suitable value according to the detected moisture content, thus facilitating standard biomass particle shaping. Due to its scalability, the moisture detection system can be widely used in similar agricultural granulators. Additionally, the calculation module, water replenishment devices, and experimental methods can be applied separately for moisture control in crops, livestock and poultry farming, and other agricultural scenarios related to moisture detection and control.

References

Abdullah M.S.M., Rahiman M.H.F., Zakaria A., Kamarudin L.M., Mohamed L. 2019. A review on moisture measurement technique in agricultural silos. Proc. IOP Materials Science and Engineering. 705: 012001. Bristol: Temple Circus.

Almaleeh A., Zakaria A., Kamarudin L.M., Rahiman M.H.F., Ndzi D.L. Ismail I. 2022. Inline 3D volumetric measurement of moisture content in rice using regression-based ML of RF tomographic imaging. Sensors-BASEL. 22(1): 405.

Agrawal N., Thakur O.P., Anjani K.S. 2021. Analysis of electromechanical properties of electrode for enhancing electrostrictive capacitive sensor response. Mater. Today. Proc. 47(8): 1621-1626.

Amer M., Nour M., Ahmed M., Ookawara S., Nada S., Elwardany A. 2019. The effect of microwave drying pretreatment on dry torrefaction of agricultural biomasses. Bioresource. Technol. 286: 121400.

Basok B., Davydenko B., Pavlenko A.M. 2021. Numerical network modeling of heat and moisture transfer through capillary-porous building materials. Materials. 14(8): 1819.

Fan L., Chai Z., Wang Y., Wang Z., Zhao Q., Qin X. 2020. A novel handheld device for intact corn ear moisture content measurement. IEEE. T. Instrum. Meas. 69: 9157-9169.

Fan W., Chen Q., Chen M. 2022. Online capacitive detection method for moisture content of aggregate based on edge effect. Measurement. 203: 111962.

Gurol I.E., Basar E., Kucukyavuz D., Onat F.A. 2022. A novel orthogonal frequency division multiplexing with index modulation waveform with carrier frequency offset resistance and low peak-to-average power ratio. Int. J. Commun. Syst. 35(7): e5094.

Han J., Guo J., Zhang Z., Yang X., Shi Y., Zhou J. 2023. The rapid detection of trash content in seed cotton using near-infrared spectroscopy combined with characteristic wavelength selection. Agriculture. 13:1928.

Hartley R., Ghaffari M., Eustice R.M., Grizzle J.W. 2020. Contact-aided invariant extended Kalman filtering for robot state estimation. Int. J. Robot. Res. 39(4): 402-430.

Li C., Zhang X., Meng M., Li B., Li C. 2021. Capacitive Online Corn Moisture Content Sensor Considering Porosity Distributions: Modeling, Design, and Experiments. Appl. Sci. 11(16): 7655.

Li L., Bo M., Xue J., Shang G., Li S. 2021. Difference in corn kernel moisture content between pre- and post-harvest. J. Integr. Agr. 20(7): 1775-1782.

Li T., Ji Y.H., Zhang M., Li M.Z. 2017. Determining optimal CO_2 concentration of greenhouse tomato based on PSO-SVM. Appl. Eng. Agric. 33(2): 157-166.

Lv W., Zhang M., Wang Y., Adhikari B. 2017. Online measurement of moisture content, moisture distribution, and state of water in corn kernels during microwave vacuum drying using novel smart NMR/MRI detection system. Dry. Technol. 36: 1592-1602.

Jain S., Mishra P. K., Mishra J., Thakare V. 2020. Design and analysis of H-Shape patch sensor for rice quality detection. Mater. Today. 29: 581-586.

Jafarpisheh N., Zaferani E.J., Teshnehlab M., Karimipour H., Parizi R.M., Srivastava G. 2021. A deep neural network combined with radial basis function for abnormality classification. Mobile. Netw. Appl. 26(6): 2318-2328.

NAMSTC, 2013. Machinery industry standard of the People’s Republic of China. JB/T 5161-2013. National Agricultural Machinery Standardization Technical Committee, Beijing, China.

Park S., Choi H. 2021. Characteristics of a superconducting DC circuit breaker according to L and C elements of LC divergent oscillation circuit. IEEE T. Appl. Supercon. 31(8), 5604604.

Sayari S., Mahdavi-Meymand A., Zounemat-Kermani M. 2021. Irrigation water infiltration modeling using machine learning. Comput. Electron. Agr. 180: 105921.

Sivtsov D.P., Khandetskyi V.S. 2015. Device to determine of fluorine concentration in fluorinated carbon powders. Syst. Technol. 1: 3-9.

Tran T.N., Lam B.M., Nguyen A.T., Le Q.B. 2022. Load forecasting with support vector regression: influence of data normalization on grid search algorithm. Int. J. Electr. Comput. 12(4): 3410-3420.

Thais L.C., Giovani A., Carlos H., Duarte C.R. 2021. Biomass feeding in a dilute pneumatic conveying system. Powder. Technol. 391: 321-333.

Vidal A.K.F., Daher R.F., Freitas R.S., Stida W.F., Lédo F.J.D.S., Silva V.B.D., Farias J.E. 2022. Growth curve in elephant grass genotypes based on morpho-agronomic traits for energy production. Chil. J. Agr. Res. 82(1): 78-87.

Wang J., Tang T., Tang H., Xu W., Zhou W., Wang Q. 2021. Design and experiment of on-line detection device for capacitive paddy rice moisture content of combine harvester. Tran. CSAE. 52(03): 143-152.

Wang X., Ma T., Yang T., Song P., Chen Z., Xie H. 2019. Monitoring model for predicting maize grain moisture at the filling stage using NIRS and a small sample size. Int. J. Agric. Biol. Eng. 12(2): 132–140.

Wang R., Xu T., Zhao J., Wang Y., Xing J., Lyu T., et al. 2020. Effects of harvest date on maize grain moisture content and grain mechanical harvesting quality. J. Agr. Scitech-Iran. 22(11): 35-41.

Wang W., Gong Y., Bai X., Tan R., Huang W. 2021. Investigation on operating speed regulation system of mobile straw granulator. Trans. CSAE. 52(10): 186-195.

Wang W., Quan X. 2023. Estimation of live fuel moisture content from multiple sources of remotely sensed data. IEEE. Geosci. Remote. S. 20: 1-5.

Wang W., Zhang S., Li J., Zhang P., Chen Y. 2022. Effects of the twin-row planter with subsoiling on soybean growth and yield in northern China. J. Agric. Eng-ITALY. LIII: 1359.

Yigit E., Duysak H. 2022. Determination of flowing grain moisture contents by machine learning algorithms using free space measurement Data. IEEE. T. Instrum. Meas. 71:1-8.

Zhou S., Bilal M., Khan M.A., Muhammad T. 2021. Numerical analysis of thermal radiative maxwell nanofluid flow over-stretching porous rotating disk. Micromachines. 12(5): 540.

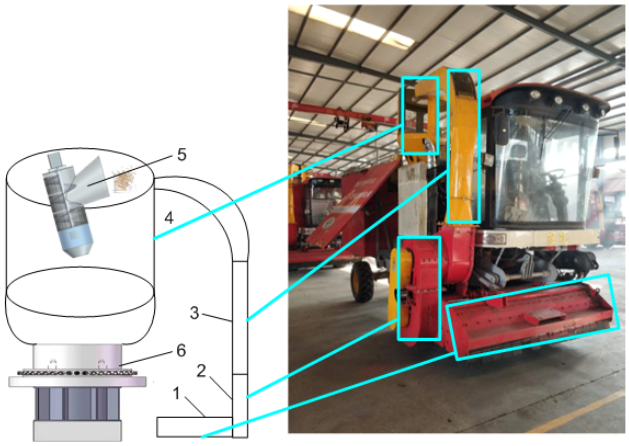

A

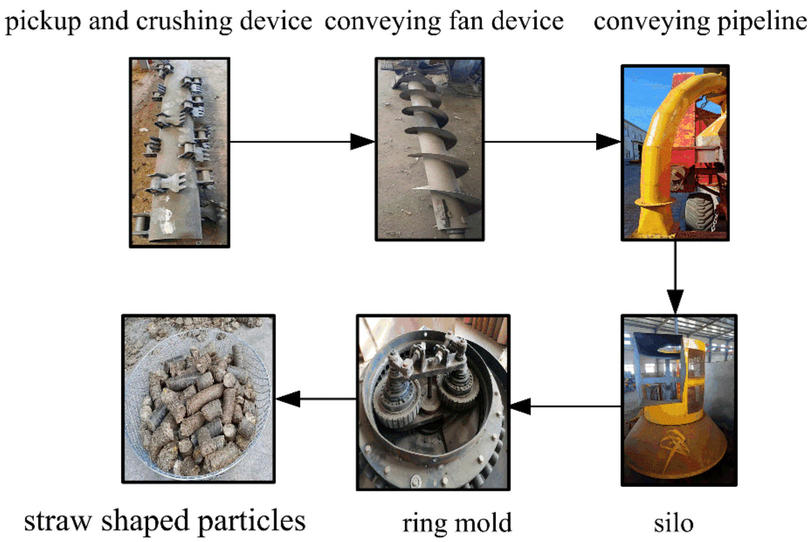

B

Figure 1. The diagram and the flow chart of the mobile straw granulator. A) The diagram of the mobile straw granulator. 1: pickup and crushing device; 2: conveying fan device; 3: conveying pipeline; 4: silo; 5: moisture content acquisition module; 6: ring mold; B) the flow chart.

A B C

Figure 2. The actual biomass particles. A) low moisture; B) normal moisture; C) high moisture.

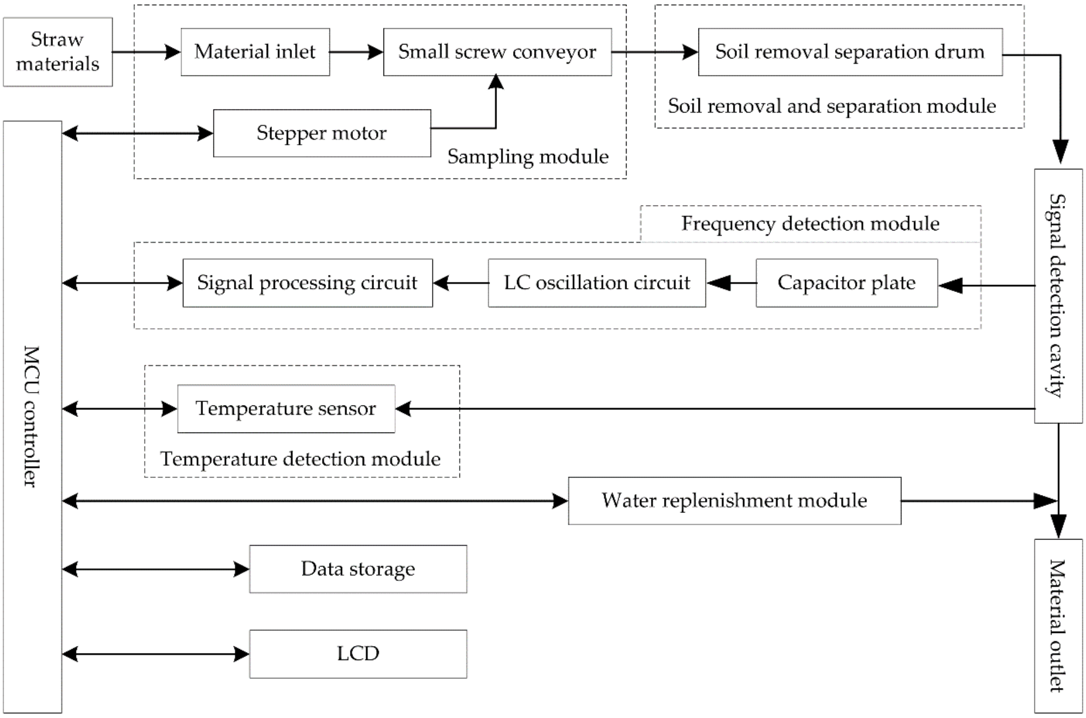

Figure 3. Block diagram of real time moisture content detection system.

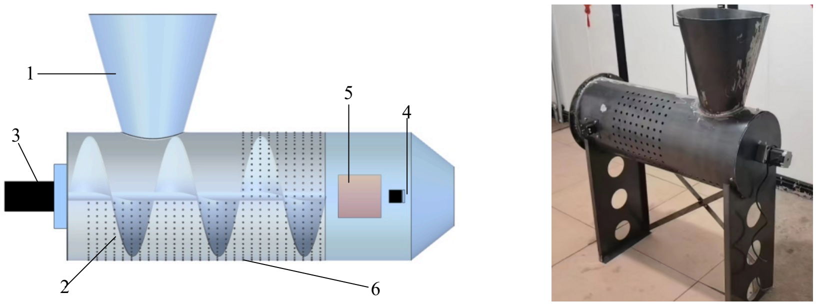

A B

Figure 4. Moisture content acquisition device. A) sketch map; 1: material inlet; 2: small screw conveyor; 3: M3 stepping motor; 4: M1 and M2 stepping motor; 5: red copper electrode; 6: signal detection chamber; B) picture of real products.

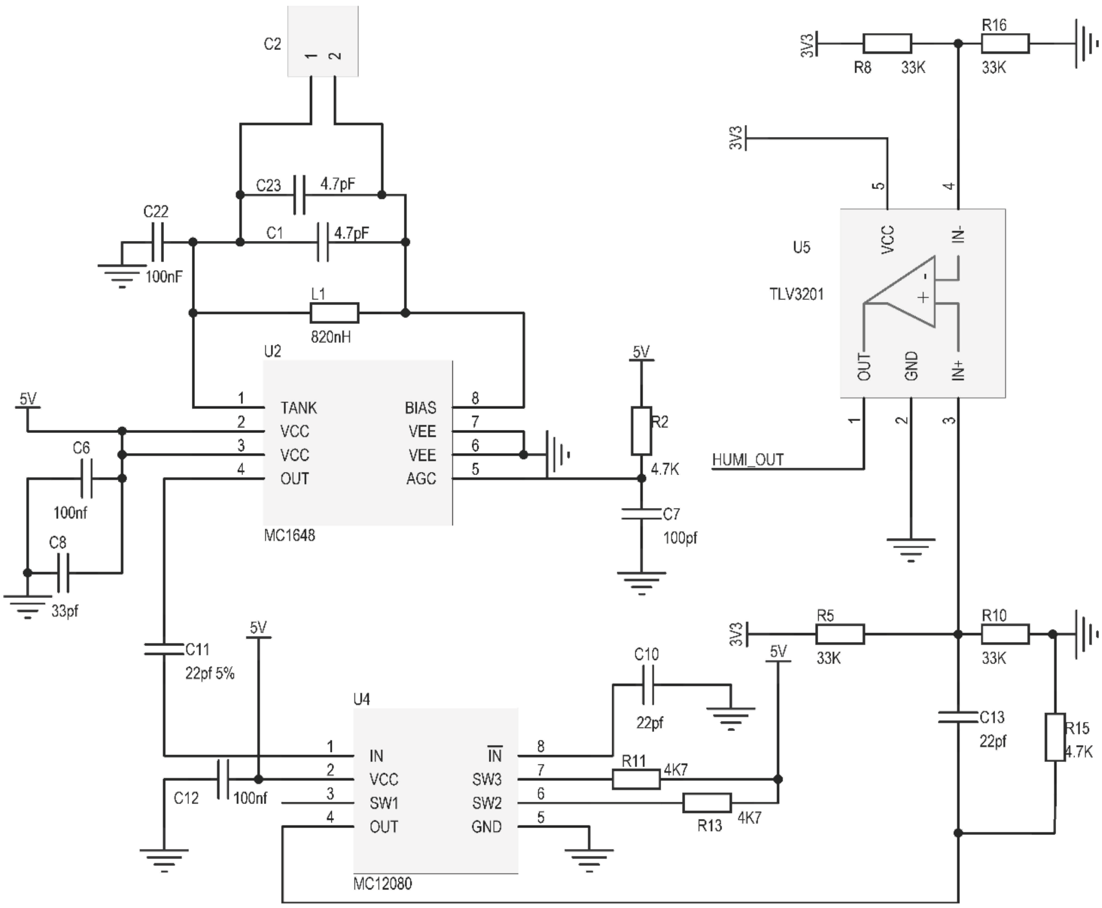

A

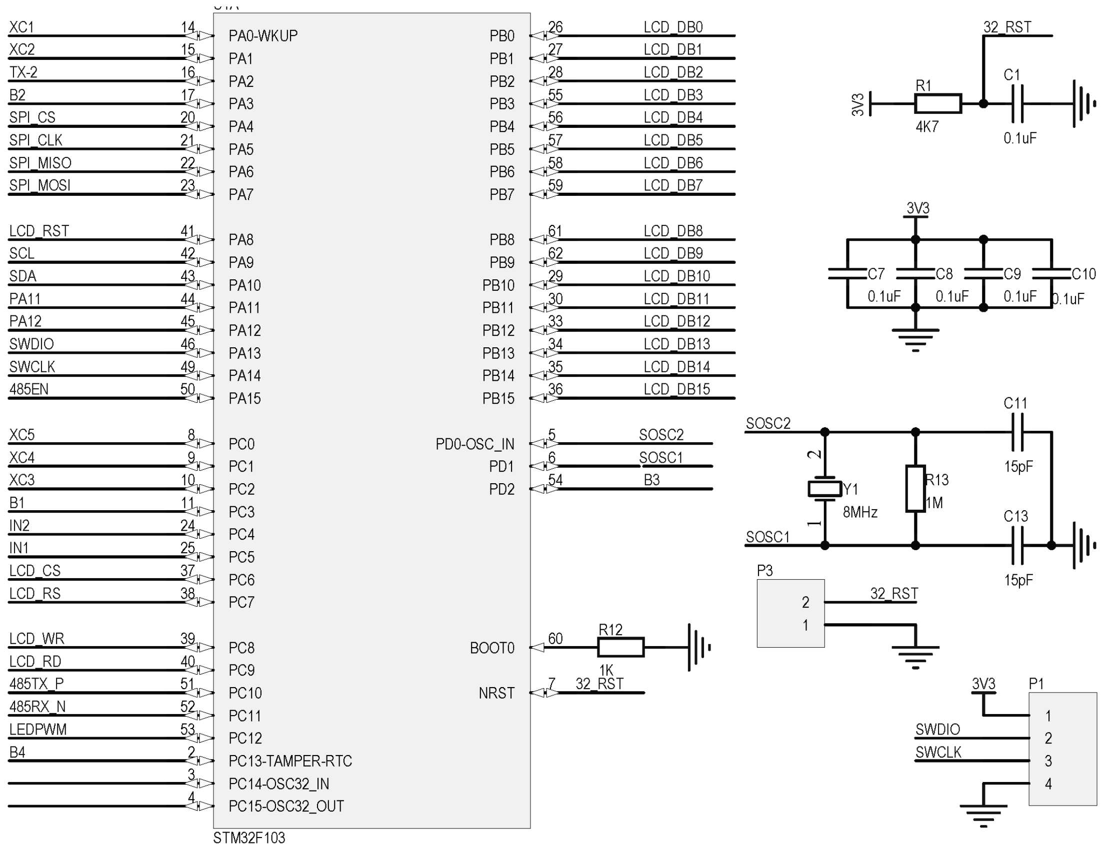

B

Figure 5. The main electronic design. A) Design of the Frequency Sensor; B) Main control module.

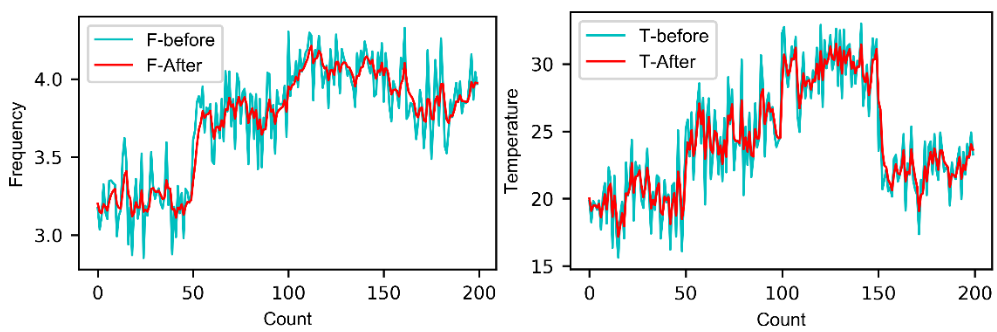

A B

Figure 6. Kalman filtering of frequency and temperature. A) Filtering data of frequency; B) Filtering data of temperature.

A B C

Figure 7. Water replenishment device. A) Water replenishment tank; B) Electric control water valve; C) Water replenishing nozzle.

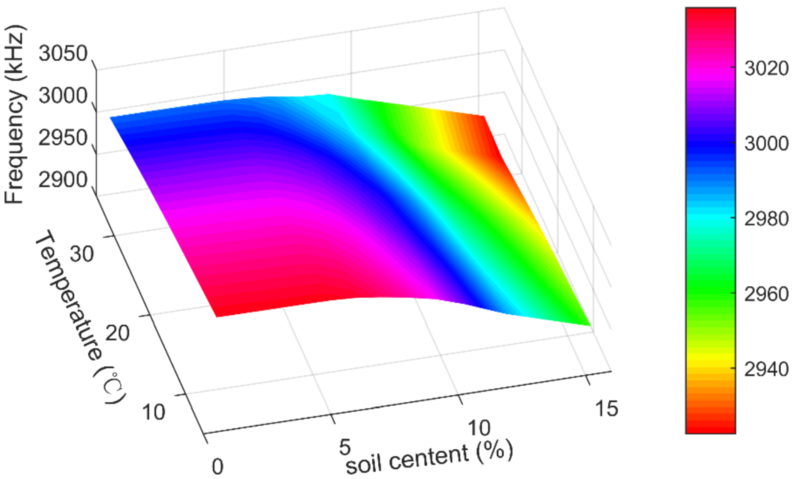

A

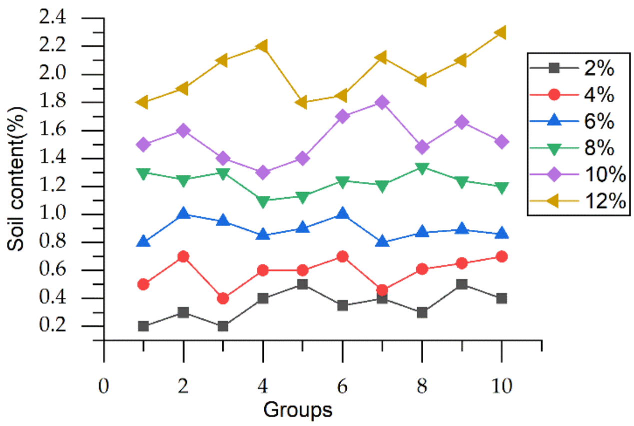

B

Figure 8. Results of the pilot tests. A) Influence of temperature and soil on frequency; B) Soil content after processed by soil separator cylinder with different initial soil content.

Table 1. Training data.

MC(%)	5 (°C)	10 (°C)	15 (°C)	20 (°C)	25 (°C)	30 (°C)	35 (°C)
9.09	4.065	4.044	4.021	4.004	3.988	3.974	3.960
13.12	3.492	3.477	3.463	3.449	3.435	3.422	3.410
17.15	3.119	3.113	3.107	3.100	3.092	3.083	3.073
20.80	3.041	3.035	3.029	3.022	3.015	3.006	2.996
25.12	2.935	2.928	2.923	2.917	2.910	2.902	2.893
28.23	2.806	2.799	2.793	2.787	2.781	2.774	2.767
33.44	2.580	2.575	2.570	2.563	2.557	2.552	2.548
37.19	2.513	2.509	2.505	2.500	2.494	2.490	2.486
43.35	2.396	2.394	2.391	2.387	2.382	2.378	2.375
46.68	2.375	2.373	2.369	2.365	2.360	2.356	2.351

MC, moisture content. First column represents the moisture content. The second to eight columns represent detected frequency corresponding to the set moisture content and temperature.

Table 2. Results of Moisture content detection and soil removal performance experiments.

GN	MC-DM (%)	SC (%)	MC-S (%)	AAE (%)	MAE (%)
1	10.12	0.85	10.19	0.07	0.11
2	20.67	1.19	20.78	0.11	0.32
3	26.28	1.21	26.43	0.15	0.27
4	32.62	1.69	32.31	0.31	0.44
5	38.42	1.72	38.09	0.33	0.39
6	40.54	1.71	40.25	0.29	0.37

GN, group number; MC-DM, moisture content obtained by 105 °C drying method; SC, soil content after removal; MC-S, moisture content obtained by the system proposed in this paper; AAE, average absolute error between MC-DM and MC-S; MAE, maximum absolute error between MC-DM and MC-S.

Table 3. Results of overall system experiment.

GN	MC-DM (%)	MC-S (%)	FA (Kg/s)	WRA(Kg/s)	MC-S-W(%)	MRN(%)	MR(%)
1	9.58	10.01	1.087	0.160	21.58	70.21	93.38
2	11.91	12.23	1.085	0.129	21.45	75.32	95.27
3	14.22	15.26	1.091	0.088	21.55	79.24	93.22
4	18.28	18.19	1.082	0.047	21.28	88.48	94.59

GN, group number; MC-DM, moisture content obtained by 105 °C drying method; MC-S, moisture content obtained by the system proposed in this paper; FA, feeding amount; WRA, water replenishment amount; MC-S-W, moisture content detected after replenished; MRN, the molding rate without the designed system; MR, the molding rate used the designed system.

Table 4. Moisture content detection experiment with straw in proper range.

GN	Fre (MHz)	Tem (°C)	Moisture Content (%)		Abs-E	Molding rate (%)
			detected	105°C dried		
1	3.034	7.0	21.07	21.32	0.25	92.35
2	3.033	8.0	21.05	21.40	0.35	93.28
3	3.035	7.0	21.02	21.39	0.37	94.29
4	3.037	7.0	20.92	21.27	0.35	93.69
5	3.034	8.0	21.00	20.59	0.41	93.43
6	3.035	8.0	20.95	20.50	0.45	94.37
Aver	3.035	7.5	21.00	21.08	0.36	93.57

GN, group number; Fre, frequency; Tem, temperature; Abs-E, absolute error.

Table 5. Moisture content detection experiment with dry straw.

G-N	Fre (MHz)	Tem (°C)	FA (Kg/s)	WRA (Kg/s)	Moisture Content (%)				Molding rate (%)
					detected	105°C dried	Abs-E	MC-S-W	
1	3.172	9.0	1.256	0.095	15.61	15.94	0.33	21.68	90.76
2	3.170	9.0	1.301	0.098	15.64	15.93	0.29	21.04	91.65
3	3.181	9.0	1.305	0.101	15.49	15.16	0.33	21.45	89.48
4	3.170	9.0	1.304	0.099	15.60	15.97	0.37	21.55	88.51
5	3.174	8.0	1.305	0.099	15.60	15.23	0.37	21.61	88.28
6	3.178	9.0	1.288	0.099	15.53	15.89	0.36	21.58	89.87
Aver	3.174	8.8	1.293	0.099	15.58	15.69	0.34	21.49	89.76

GN, group number; Fre, frequency; Tem, temperature; FA, feeding amount; WRA, water replenishment amount; Abs-E, absolute error; MC-S-W, moisture content detected after replenished.